doi.org/10.36721/PJPS.2022.35.5.REG.1423-1436.1

Study on the nasal drug delivery system of PPX microcapsules *in situ* thermosensitive gel

Lin Ma[1], Yang Zhao[1], Tianyang Li[1], Jingshu Piao[1]* and Mingguan Piao[1,2]*
[1]School of Pharmacy, Yanbian University, Yanji, China
[2]Key Laboratory of Natural Medicines of the Changbai Mountain, Ministry of Education, Yanbian University, Yanji, China

Abstract: Pramipexole hydrochloride (PPX) is a dopamine receptor agonist for the treatment of Parkinson's disease. It does not penetrate easily into the brain due to the presence of the blood-brain barrier (BBB), which hinders the treatment of the disease. The nasal mucosal drug delivery system is an effective method to deliver drugs to the brain bypassing the blood-brain barrier and the concentration of drugs targeted to the brain by intranasal administration is quite low due to the limitation of the permeability of the nasal mucosa and the nasal environment. Therefore, this study innovatively encapsulates prepared PPX microcapsules in a temperature-sensitive *in situ* gel for intranasal drug delivery to increase the target concentration of the drug in the brain and prolong the duration of treatment. The gel formulation containing 24% poloxamer 407 and 6% poloxamer 188 and 0.3% ice chips as absorption enhancers formed a hard gel at 30.44-31.36^{o}C and allowed a slow release within 12 hours. A pharmacokinetic comparison of the developed PPX microencapsulated temperature-sensitive *in situ* gel (PPX-MTISG) with PPX temperature-sensitive *in situ* gel (PPX-TISG) revealed that the microencapsulated nasal mucosal *in situ* gel was a more effective PPX brain-targeted drug delivery system.

Keywords: PPX, microcapsules, *in situ* gel, nasal delivery, brain-targeted.

INTRODUCTION

Parkinson's disease (PD) is a chronic progressive neurodegenerative disorder characterized by early and prominent death of dopaminergic neurons in the substantia nigra pars compacta (SNpc) and a wide spread presence of alpha synuclein (aSyn), an intracellular protein (Radhakrishnan *et al*., 2018), its cause is enigmatic for most individuals (Samii *et al*., 2004). As the second most common neurodegenerative disease among the elderly, the incidence of Parkinson's disease is increasing and it shows a trend of younger age (Wang *et al*., 2020). The burden of PD is a growing health-care problem, with a global prevalence that is expected to double from 6.2 million cases in 2015 to 12.9 million cases by 2040 (Dorsey *et al*., 2018). Drug therapy is the first choice of PD. Common therapeutic agents include dopamine precursors, dopamine receptor agonists, drugs to inhibit dopamine metabolism and drugs to promote dopamine release (Wang *et al*., 2020). PPX is a non-ergoline dopamine D3 receptor agonist (McCormick *et al*., 2015) and is an FDA approved drug for the treatment of PD. It is effective in treating motor symptoms at various stages of Parkinson's disease and can also improve depressive symptoms. Although there are more anti-PD drugs, due to low levels of plasma exposure and the drug efflux properties of neuronal cells, orally delivering anti-PD drugs is challenging (Liu *et al*., 2020). Also, since PPX half-life ($t_{1/2}$) is 8-12h, patients need to take immediate release formulation three times daily, resulting in poor patient compliance in addition to the fluctuation of blood drug concentration.

The nasal epithelium is the only non-invasive access to all regions of the central nervous system (Rassu *et al*., 2015). The nasal drug delivery system allows direct drug delivery to the brain, allowing the drug to bypass the blood-brain barrier. It also avoids first-pass metabolism in the gastrointestinal tract and the liver. Nasal doses are typically 2 to 10 times lower than oral doses (Mahajan *et al*., 2014). Recently, several studies have demonstrated the effectiveness of intranasal delivery systems, including levetiracetam (Gonçalves *et al*., 2019), lactoferrin (Lf)-modified nanoparticles loaded with amphiphilic MnP (Lf-NP-MnP) (Matsuho *et al*., 2017), lamotrigine (Serralheiro *et al*., 2015) and kaempferol (KPF) (Patil *et al*., 2006; Mahajan *et al*., 2009; Colombo *et al*., 2018). However, nasal mucociliary clearance (NMCC) acts as the main limiting factor for nasal drug delivery and the effective adsorption time of the drug in the nasal cavity depends mainly on it. This is because nasal mucosal cilia clearance limits the time of drug absorption (Merkus *et al*., 1998). Therefore, when a clinically safe and effective intranasal drug formulation is developed, nasal mucosal clearance needs to be taken into consideration. To prevent rapid clearance of mucus cilia and to prolong dwell time, a thermally reversible *in situ* gel system was used. Temperature-sensitive *in situ* gel delivery systems have emerged as one of the best new drug delivery systems with unique "sol-gel" transition properties that facilitate sustained and controlled drug release and ensure prolonged contact time with the nasal mucosa, reduce mucosal dripping, anterior leakage and clearance after drug administration and promote drug absorption (Singh *et al*., 2013; Nižić *et al*., 2019; Teaima *et al*., 2020). Therefore, it is particularly useful for long-term use of drugs (Salunke *et al*., 2016). Traditional intranasal drug delivery systems (e.g., solutions, suspensions and ointments) show disadvantages such as short intranasal

**Corresponding author:* e-mail: mgpiao@ybu.edu.cn

residence time, inconvenient administration and low permeability compared to them (Choi *et al*., 2017; Pidaparthi *et al*., 2017). Moreover, considering innovative mucus delivery systems and appropriate delivery modalities are reasonable and beneficial strategies to improve the therapeutic outcomes of nasal drug delivery. In this study, polymeric microspheres encapsulated into temperature-sensitive *in situ* gels as dry powder formulations are promising nasal delivery systems with many advantages in terms of liquid formulations, including delayed mucus cilia clearance, higher drug concentration at the deposition site and better stability (Prajapati *et al*., 2008; Bah *et al*., 2020; Nižić *et al*., 2020).

Poloxamer is a synthetic long-chain polyoxyethylene-polyoxypropylene-polyoxyethylene block polymer with biocompatible properties, PLO has the advantage of biocompatibility and semi-solid consistency suitable for application in defined skin areas (Ahmed *et al*., 2019; Zarrintaj *et al*., 2020). Poloxamer 407 has excellent thermosensitive gelling properties. Poloxamer 407 is composed of ethylene oxide (EO) and propylene oxide (PO). The gelation mechanism of Poloxamer 407 is related to the critical micelle concentration (CMC) and critical micelle temperature (CMT) (Machado *et al*., 2013; Akkari *et al*., 2016; Giuliano *et al*., 2018). However, the gel conversion temperature of Poloxamer 407 is very low, so this paper chooses to combine Poloxamer 407 and Poloxamer 188 for nasal mucosal administration research.

In this study, PPX hydrochloride was encapsulated into microspheres and the microcapsule materials were also screened by drug loading and *in vitro* cumulative release percentage; the prescription was screened by drug loading and *in vitro* cumulative transmission rate. We not only evaluated the quality of the final prepared temperature-sensitive gels, but also investigated the pharmacokinetic behavior of the microencapsulated temperature-sensitive *in situ* gel of PPX hydrochloride for nasal administration. The focus of this article is to use the emulsification solvent evaporation method to encapsulate the drug in the microcapsules, to prepare the temperature-sensitive *in situ* gel by the condensation method and to disperse the microcapsules into the optimized gel formulation to increase the concentration of the drug targeted to the brain. The formation process of the in-situ gel is shown in fig. 1.

MATERIALS AND METHODS

Poloxamer 407, Carbomer, Lecithin, Polylactic acid were purchased from Wuhan far Cheng Co-Creation Technology Co., Ltd. (Wuhan, China), Poloxamer 188 was purchased from Nanjing Well Chemical Co., Ltd. (Nanjing, China), Borneol, Tween 80, Ascorbic acid, Ethylparaben, Span 80, Ethylcellulose were purchased from Shanghai Aladdin Biochemical Technology Co., Ltd. (Shanghai, China), Polyvinyl pyrrolidone was purchased from Anhui Sun here Pharmaceutical Excipients Co., Ltd. (Anhui, China), Hyaluronic acid was purchased from Zhenjiang Dongyuan Biotechnology Co., Ltd. (Jiangsu, China), PPX dihydrochloride was purchased from Finetech Technology Co., Ltd. (Wuhan, China). All other reagents were of at least analytical grade.

Preparation and optimization of PPX microcapsules

Preparation of PPX microcapsules

PPX microcapsules were prepared with the conventional emulsion solvent evaporation method. Take an appropriate amount of capsule material into acetone and conduct an ultrasonic treatment to dissolve it. The liquid paraffin and Span 80 were mixed evenly by a magnetic stirrer (HJ-2A, Jintan, China). At a certain temperature and speed, a peristaltic pump (L100-1S-1, Shanghai, China) was used to slowly drip the liquid paraffin phase into the acetone phase and a suitable amount of 1,2-propanediol was added. Then the system was stirred at a certain speed until the organic solvent was volatilized. Microcapsules were collected by vacuum filtration (SHZ-DIII, Gongyi, China) and then washed three times with n-hexane and dried in a blast drying oven (DHG-9243B5-III, Shanghai, China) at 40 ^{o}C for 12 h (Feng *et al*., 2018). The composition of the formulation is shown in table 1.

Prescription screening of microcapsules

Screening of capsule material

In this experiment, the drug loading and *in vitro* cumulative release rate were used as evaluation indexes to evaluate the microcapsules prepared by using three different capsule materials. The preparation method was as follows emulsion solvent evaporation method.

Precisely weigh 5 mg of the three samples prepared by the above method and add 5 mL of ethanol, respectively. Then shaken with full-temperature shaker (GHA-E, Changzhou, China) for 3 days, the samples were filtered by a 0.45 μm millipore filter. The drug loading percent was determined by UV-VIS spectrophotometry. The drug load is calculated by the Equation 1 (Wang *et al*., 2021).

$$LE(\%) = \frac{W_e}{W_{m\times 100\%}} \quad \text{Eq. 1.}$$

In the formula, LE represents the percentage of drug loading in the microcapsule; W_e denotes the amount of drug encapsulated in the microcapsule; W_m represents the total weight of the drug-carrying microcapsules.

In vitro release experiments were conducted using a dissolution tester (RCZ-6B3, Shanghai, China). The dissolution medium was distilled water (500 mL), the rotational speed in the experiment was 100 r·min^{-1}, the temperature in the experiment was (37±0.5)^{o}C and 5 mL was taken at 10, 20, 30, 60, 90, 120, 180, 240, 360, 540, 720 min, respectively. And add the same volume medium at the same temperature, over 0.45 μm microporous filter

membrane. The detection wavelength was 262 nm and the cumulative release rate was calculated. The cumulative *in vitro* release rate was calculated by the Equation 2.

$$Q = \frac{\sum_{i=1}^{n-1} C_i V_i + C_n V}{M} \times 100\% \quad \text{Eq. 2.}$$

In the formula, C_1 is the drug mass concentration measured at the first sampling point, C_n is the drug mass concentration measured at the NTH sampling point ($n \leq n-1$), V_1 is the volume of dissolution release medium, V is the sampling amount and M is the drug amount added to the preparation.

Prescription composition screening

Microcapsules were prepared according to the prescription composition in table 1. The preparation method was as follows emulsion solvent evaporation method. In this experiment, drug loading percent and cumulative penetration *in vitro* were selected as evaluation indicators.

The method for determination of drug loading rate is the same as that mentioned in screening of capsule material.

The cumulative penetration *in vitro* was measured by the Franz transdermal diffusion apparatus. The nasal mucosa was replaced by the small intestine of rabbits and NFS was used as the receiving fluid. The rotational speed was 200 r·min^{-1} and the temperature was 37±0.5°C At 15, 30, 45, 60, 90, 120, 180, 240, 300, 360, 540, 720 min, 5mL was taken from the membrane and 5 mL NFS was added. The samples were filtered by a 0.45 μm millipore filter. The detection wavelength was 262nm. The cumulative penetration *in vitro* was calculated by HPLC.

Each prescription sample was prepared according to the formulation composition of PPX hydrochloride microcapsules in table 1 and the preparation method was 2.2.1. Prescriptions were screened using drug loading and *in vitro* cumulative throughput as evaluation indexes.

Five kinds of microcapsule samples prepared with different prescriptions were accurately weighed, 5 mg were added with 5mL of ethanol, shaken for 3 days on a full-temperature shaker (GHA-E, Changzhou, China), then filtered through 0.45μm microporous membrane, the filtrate was taken for UV determination and drug loading was calculated.

The Franz transdermal diffuser (TP-6, Tianjin, China) was used to measure the cumulative penetration *in vitro*. A rabbit small intestine was used to replace the nasal mucosa. Place the rabbit's small intestine between the supply room and the receiving room. The volume of the receiving room is 15 mL. The stirring speed was set at 200 rpm and the solution temperature was set at 37.0±0.5°C. After 15 min, equilibrium was started.

After 15, 30, 45, 60, 90, 120, 180, 240, 300, 360, 540 and 720 min, 5 mL of the sample was taken and the isothermal and equal volume solution was added and the 0.45μm microporous membrane was filtered. The drug concentration was determined by HPLC. The detection wavelength was 262 nm and the cumulative transmittance is calculated by the Equation 3.

$$Q_n = [C_n \bullet V + V_o \sum_{i=1}^{n-1} C_i]/A \quad \text{Eq. 3.}$$

Characterization of microcapsules

The morphological examination of microcapsules was performed by Transmission Electron Microscopy (HT-7700, Hitachi, Japan) and by Scanning Electron Microscopy (SU-8010, Hitachi, Japan), respectively. The dried microcapsule powder was coated with gold palladium under an accelerated voltage of 15 KV in argon atmosphere. Sputtering was done for 3 minutes to record SEM (Dai *et al*., 2020). The sample was dropped onto a copper mesh with carbon film and after drying, it was observed on a TEM under an acceleration voltage of 80 KV (Shen *et al*., 2017).

Preparation and optimization of in situ thermosensitive gel

Preparation of in situ thermosensitive gel

In this experiment, the temperature-sensitive in-situ gel was prepared by the cold storage method (Zhan *et al*., 2019). Added the proper amount of absorption enhancer, biological adhesives, antioxidants, bacteriostats, Poloxamer 188 and Poloxamer 407 to distilled water (Gu *et al*., 2020). High shear dispersing emulsifier (FM-200, Shanghai, China) was used to make the mixture evenly and then it was placed at 4℃ for 24 h.

Optimization of in situ thermosensitive gel

Optimization of gel matrix Poloxamer 407 and Poloxamer 188

In this experiment, gel temperature (T_{gel}) and gel dissolution mass were used as evaluation indexes to screen the content of gel matrix.

T_{gel} determination method (Jin *et al*., 2009; Shao *et al*., 2009): place 4 mL gel solution in a test tube, insert the thermometer, place the test tube in the water bath and gradually heat 1°C per minute. T_{gel} is the temperature at which the contents do not flow when the tube is tilted 90°. All experiments were performed in triplicate.

Gel dissolution method: An appropriate amount of gel solution was added to a flat-bottomed vial and preheated in a water bath at 37°C. After the gel was formed, 5 mL of releasing medium artificial nasal fluid (NFS) was slowly added to the surface of the gel along the inner wall of the vial. Then the vial was placed in a thermostatic shaker with the rotating speed set at 100 r·min^{-1} and the temperature set at (37±0.5)°C Every 1 hour, remove all release media, record vial mass and supplement with 5 mL of NFS. The mass difference of adjacent time points is the mass of gel dissolution in this time period.

Optimization of the content and species of biological adhesives

In this experiment, the content and types of biological adhesives were screened using the adhesive strength as the evaluation index.

Method for determination of adhesion strength: The self-made experimental device is shown in fig. 2. The glass plate was placed in the water bath at 37°C for 10 min. Apply the appropriate amount of gel evenly onto the glass plate, then cover the glass for 10 min and hang the beaker with a pulley to maintain balance. Gradually add weight to the beaker until the cover slide is detached. Recorded the mass of the beaker at this time and substituted the adhesion strength formula.

Adhesion strength (dynes·cm^{-2}) = 980 × m/A…….Eq. 4.
m: mass of weight (g), A: area of the cover glass (cm^2)

Adhesion strength was determined by adding 0.25%, 0.35% and 0.45% biological adhesive, respectively. When the volume fraction was constant, three kinds of biological adhesives, including polyvinyl ketone, carbomer and hyaluronic acid, were added respectively and their adhesion strength was measured.

Optimization of content and types of absorption accelerator

In this study, the content and types of absorption promoters were screened using the cumulative drug penetration as the evaluation index. Preparation of mucosa required for membrane diffusion: nasal mucosa is required for this experiment, but it cannot be used because the nasal mucosa is too small after dissection and the physiological characteristics of the small intestine are very similar to the mucosa and easy to obtain, so the rabbit small intestine was selected to replace the nasal mucosa in this experiment. The method for determining cumulative transmittance is the same as indicated under screening of capsule material.

The effects of different volume fractions of absorption promoters of 0.1%, 0.2% and 0.3% on the cumulative transmittance were measured. When the volume fraction was 0.3%, three absorption promoters of Borneol, Twain-80 and Lecithin were added, respectively and the cumulative transmittance was measured.

Quality Evaluation of in situ thermosensitive gel

Percent of drug content

The percent of drug content was determined by T_{gel} and gel dissolution. The determination method was the same as Optimization of Gel matrix Poloxamer 407 and Poloxamer 188.

Basic properties of in situ thermosensitive gel

Gel temperature

The T_{gel} temperature test method was the same as that used in Optimization of *in situ* Thermosensitive Gel experiment.

Gel spreading

Measurement of spreading ability (Dahlizar *et al*., 2018): the small intestine of rabbits was laid flat on an 18 cm×3 cm rectangular glass plate and placed in an electrothermal, thermostatic blast drying oven at 37°C for 5 min. One drop of *in situ* gel solution was dropped on the small intestine and the glass plate was tilted 120° at the same time. The sliding distance of the gel before gelation was recorded.

The basic properties of this experiment include T_{gel}, gel adhesion strength, t_{gel}, pH, gel viscosity and spreadability.

The T_{gel} temperature test method was the same as that used in Optimization of *in situ* Thermosensitive Gel experiment， and the gel adhesion strength was measured by means of the apparatus as in fig. 2

Took 3-4 mL of gel solution in the test tube and then put the test tube in 37±0.5°C thermostat water bath. T_{gel} was the time requires that the test tube tilts 90° and the content did not flow.

The measurement method of spreadability is as follows. The rabbit intestines were spread on a glass plate and placed in an Electro-thermostatic blast oven at 37°C for 5 min and 1 drop of solution was dripped onto the small intestine. At the same time, the glass plate was tilted 120° and the distance of the gel passed before gelation was recorded.

Membraneless dissolution

The method of determination of gel solubility was consistent with the method of determination of solubility mentioned in the screening experiment of microcapsule prescription. Samples were taken at 15, 30, 45, 60, 90, 120, 180, 240, 300, 360 and 720 min respectively. The detection wavelength was 262 nm. The membraneless dissolution *in vitro* was calculated by HPLC.

Measurement of cumulative penetration in vitro

In vitro cumulative permeability was determined by the same Franz transdermal diffuser method used in the Prescription Composition Screening experiments. Samples were taken at 15, 30, 45, 60, 90, 120, 180, 240, 300, 360 and 720 min respectively. The drug content was determined by HPLC after the release medium was taken out and the cumulative penetration was calculated.

Pharmacokinetic evaluations of developed Pramipexole Hydrochloride Temperature Sensitive Gel

The *in situ* thermosensitive gels were evaluated for the delivery of PPX into systemic circulations and brains of

SD rats via the intranasal route. Forty-eight healthy SD rats (male) were randomly divided into two groups (n = 3 per group). The rats in the experimental group were given with PPX-MTISG and the control groups were given PPX-TISG.

The two groups were given intranasal administration and instilled slowly in the nose through a polyethylene tube connected to a microsyringe (Barakat *et al*., 2006; Liu *et al*., 2018). Blood samples were collected at 0.5, 1, 1.5, 2, 4, 6, 8, 12h post-dosing from the carotid artery. After centrifugation at 8000 rpm for 15 min, plasma samples were obtained for analysis. To investigate PPX brain uptake, another batch of rats were used and the animals were sacrificed at 0.5, 1, 1.5, 2, 4, 6, 8, 12 h and collected brain. All collected brain samples were stored at -20^{o}C until they were analyzed. Drug concentration was analyzed by HPLC. The PPX parameters were calculated by WinNonlin in this experiment.

Ethical approval

All animal care and experimental procedures were carried out in accordance with the guidelines of the Animal Care Committee of Yanbian University (resolution number 201501022) and were approved by the Animal Research Committee of Yanbian University, China. The animals were treated humanely and all efforts were made to minimize the animals' suffering and the animal numbers. The mice were housed under standard conditions (12/12-h light-dark cycle, temperature 25°C, 55% humidity and under SPF conditions). The mice were housed four or five per cage in plastic cages with soft bedding and supplied with standard food and water adlibitum.

RESULTS

Optimization of the microcapsules formulation

Screening of capsule material

The results of the cumulative release *in vitro* of the three samples are shown in fig. 3.

Combining with fig. 3A and fig. 3B, it can be concluded that When polyacrylic resin is used as a capsule material, the drug load is moderate and the cumulative release rate is the largest, The selected model of polyacrylic resin is Eudragit S, which has a continuous hydrocarbon chain structure, which is not absorbed by the body, does not participate in the physiological metabolism of the body and has low human toxicity. It is mainly used for microcapsule film forming agent, capsule shell film forming agent and Sustained-release preparation, so Eudragit S was chosen as the capsule material in this experiment (Jain *et al*., 2020). So polyacrylic resin is used as capsule material.

Prescription composition screening

The result of the optimization of the formulation is shown in fig. 4. Prescription screening is completed by single factor investigation, two factors: the dosage is to investigate the capsule material and Span-80 (%) to determine the process parameters. table 1 shows the composition of the microcapsule formulations, which are screened using drug loading and cumulative *in vitro* permeation as indicators. When the amount of capsule material added is 0.10g and Span-80 (%) is 1.50, the drug loading and cumulative *in vitro* permeation are the highest, drug loading is 12.27% and the cumulative permeability is 410.57μg/cm^2. Therefore, prescription V is selected as the optimal prescription.

Characterization of microcapsules

According to the image results of the scanning electron microscope and transmission electron microscope, the prepared PPX hydrochloride microcapsules were round and quasi-spherical and the surface was smooth. Therefore, the successful preparation of microcapsules can be concluded.

Optimization of the gel matrix

Screening of the content of P407 and P188 in gel matrix

When Poloxamer 188, biological adhesive and absorption enhancers were fixed, 18%-30% Poloxamer 407 was added to determine the T_{gel} and gel dissolution. As shown in fig. 6, when the Poloxamer 407 volume fraction increased, the T_{gel} decreased and the gel dissolution percent decreased. When it was 30%, the gel dissolution percent was the smallest.

When Poloxamer 407 was 30%, the biological adhesive and absorption enhancer were certain. T_{gel} increased with the increase of Poloxamer 188, but when it reached 14% and 18%, there was an insoluble gel in the solution.

When Poloxamer 407 was at 26%, biological adhesive and absorption enhancer were fixed. When the percent of Poloxamer 188 increased, T_{gel} increased first and then approached a steady state. However, when it reached 18%, there was an insoluble gel in the solution. At 10%, T_{gel} was 27.60±0.24^{o}C, which was closer to the nasal temperature.

When Poloxamer 407 was 24%, biological adhesive and absorption enhancer was certain, the T_{gel} and gel dissolution was determined by adding 2%-18% Poloxamer 188. When the Poloxamer 188 percent increased, T_{gel} first increased and then decreased. However, when the percent of Poloxamer 407 was 14% and 18%, insoluble gel appeared in the solution, while at 6% and 10%, T_{gel} was 27.50±0.08℃ and 29.57±0.12^{o}C, which were closer to the nasal temperature. Therefore, three groups of formulations shown in table 2 were initially identified.

According to the three sets of prescriptions in table 2 evaluated gel dissolution tests. The results are shown in fig. 8. Combining with T_{gel} in table 2, the best formulation was 24% of Poloxamer 407 and 6% of Poloxamer 188.

Optimization of biological adhesive

The results of adhesion strength measurement are shown in fig. 9A. When the percent of biological adhesive reached 0.45%, the adhesion strength was the highest. Therefore, the percent of biological adhesive was determined to be 0.45%.

When the percent was fixed, three kinds of biological adhesives including polyvinyl ketone, carbomer and hyaluronic acid were added and their adhesive strength was measured. The results showed that the adhesive strength of carbomer was significantly better than that of the other two species, as shown in fig. 9B.

Optimization of absorption enhancer

As shown in fig. 10A, there is no significant difference in the cumulative permeation between 0.1% and 0.2% of the absorption enhancer, while the cumulative permeation of 0.3% of the absorption enhancer is significantly higher than the former two, so the content of the selected absorption enhancer is 0.3%. Borneol was chosen as an absorption enhancer.

Quality Evaluation of in situ thermosensitive gel

Determination of the percentage range of drugs

As shown in table 3, when the percent of gel containing drug increases, T_{gel} increases first and then decreases and the percent of dissolution decreases. Combined with table 3 and fig. 11, the percentage of gel containing drugs ranged from 0% to 8%.

Determination of basic properties of temperature-sensitive in-situ gels

The results of the determination of various properties are shown in table 4.

Determination of membrane-free dissolution

The results of membrane less dissolution are shown in fig. 12. The figure shows that the gel has less gel dissolution percent. But the cumulative drug release was relatively complete and the linear trend of the two was different. It showed that the drug in the gel was mainly released by diffusion rather than gel dissolution.

Determination of cumulative in vitro penetration of drugs

The results of *in vitro* cumulative permeation are shown in fig. 13.

Pharmacokinetic evaluations

The drug concentrations in plasma and brain were determined by the internal standard method and the internal standard was domperidone and the equation of the calibration curve in plasma was y=0.0556x+0.0028 with an R^2 value of 0.9927. The equation of the calibration curve in brain was y=0.0821x+0.0035 with an R^2 value of 0.9972. intranasal PPX-MTISG had a significantly ($p<0.05$) higher PPX plasma concentration was significantly ($p < 0.05$) higher than intranasal PPX-TISG. The fig. 14A shows the variation curve of blood concentration of PPX hydrochloride with time and its equivalent pharmacokinetic parameters are shown in table 5. The C_{max} (μg/mL) of PPX-MTISG (0.44±0.12) was 1.13 times higher than that of PPX-TISG (0.39±0.23) and the AUC (μg·h/mL) of PPX-MTISG (1.89±0.99) was higher than that of PPX-MTIS (1.58±0.89) was 1.20 times higher.

Meanwhile, the $T_{1/2}$ of PPX-MTISG increased to 7.09±0.98 h and the T_{max} (h) of PPX-MTISG (1.00±0.68) was 0.5 h earlier than that of PPX-TISG (1.50±0.76), indicating that the prolonged release of drug by diffusion through the swollen polymer matrix after encapsulation in microcapsules has prolonged therapeutic effect and the potential to improve patient complian (Nižić *et al*., 2020).

Similarly, the results of drug concentration measured in the brain after intranasal administration of PPX-MTISG and PPX-MTIS showed that the C_{max}/h (μg/mL) of PPX-MTISG (0.30±0.11) was 1.67 times higher than that of PPX-MTIS (0.18±0.10) and the AUC (μg·h/mL) of PPX-MTISG (1.57±0.93) was higher than that of 2.31 times that of PPX-MTIS (0.68±0.86). Also the $t_{1/2}$ (h) of PPX-MTISG in the brain (6.72±2.31) was 1.28 times that of PPX-MTIS (5.27±1.98). This may be due to the better controlled release of the drug obtained after encapsulating the microcapsules in the gel, making the half-life of PPX-MTISG higher than that of PPX-MTIS.

Importantly, the reason why the C_{max}/h, AUC (μg·h/mL) of PPX-MTISG was higher than that of PPX-MTIS in the brain may be due to the addition of ice chips as absorption during the preparation of the microcapsules promoter, which resulted in higher drug concentration through the nasal mucosa after drug release (Liu *et al*., 2021).

DISCUSSION

Optimization of absorption enhancer

When making absorption promoter selections, as shown in fig. 10B, the three selected absorption enhancers have no significant effect on the cumulative amount of permeation, but because the drug in this study mainly acts on the brain, the absorption enhancer used in the test, Borneol, as a natural drug, not only has anti-inflammatory, anti-oxidant and anti-aging effects.

It can improve energy metabolism and promote drugs to enter target organs or tissues through various physiological barriers such as blood-brain barrier (BBB), mucous membranes and skin. Therefore, it has a significant therapeutic effect on various cardiovascular diseases, which has been confirmed by a large number of studies (Liu *et al.,* 2021). Therefore, Borneol was chosen as an absorption enhancer.

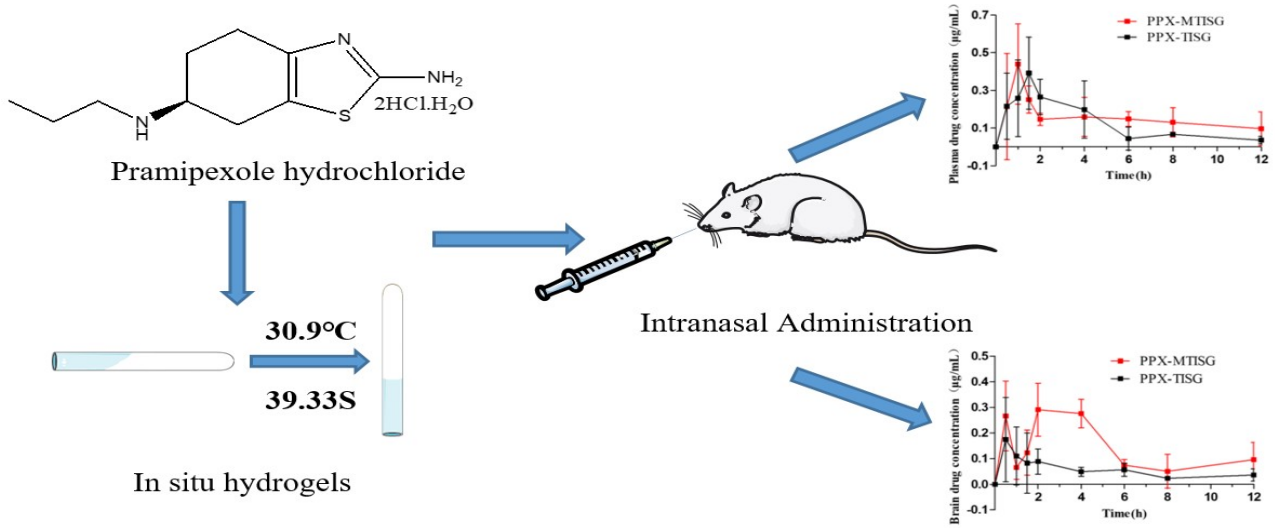

Graphical Abstract

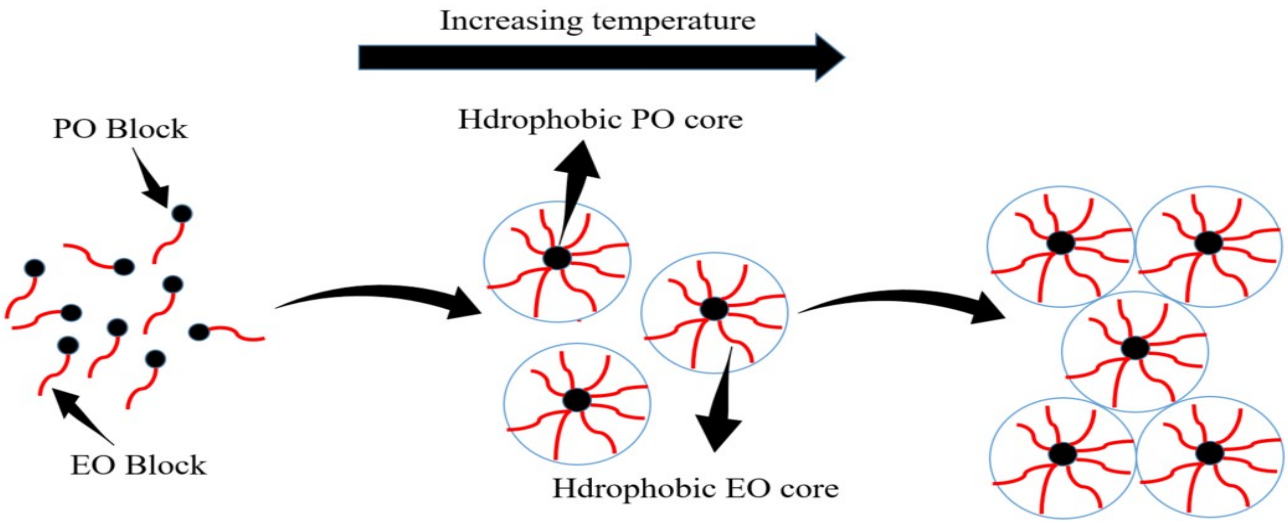

Fig. 1: *In-situ* gel and formation process**.**

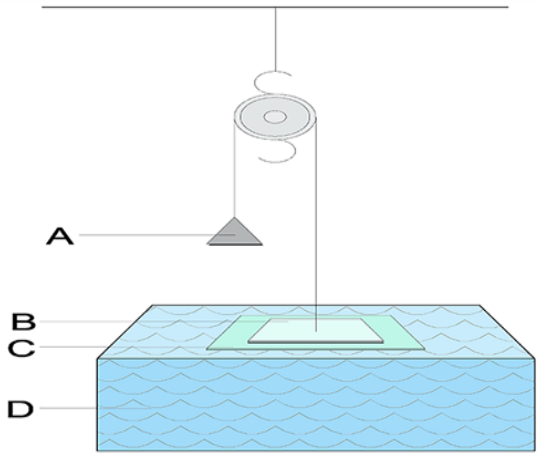

Fig. 2: Schematic diagram of the adhesion strength device.
A. Beaker; B. Cover glass; C. Glass pane; D. Thermostatic water bath

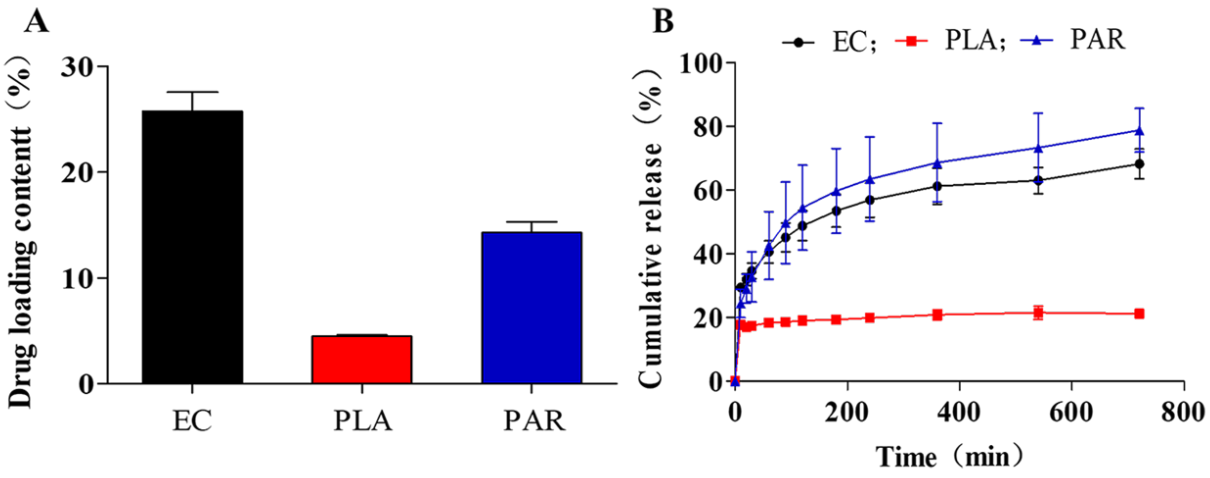

Fig. 3: (A) Drug loading of different capsule material samples; (B) cumulative release of different capsule material samples.

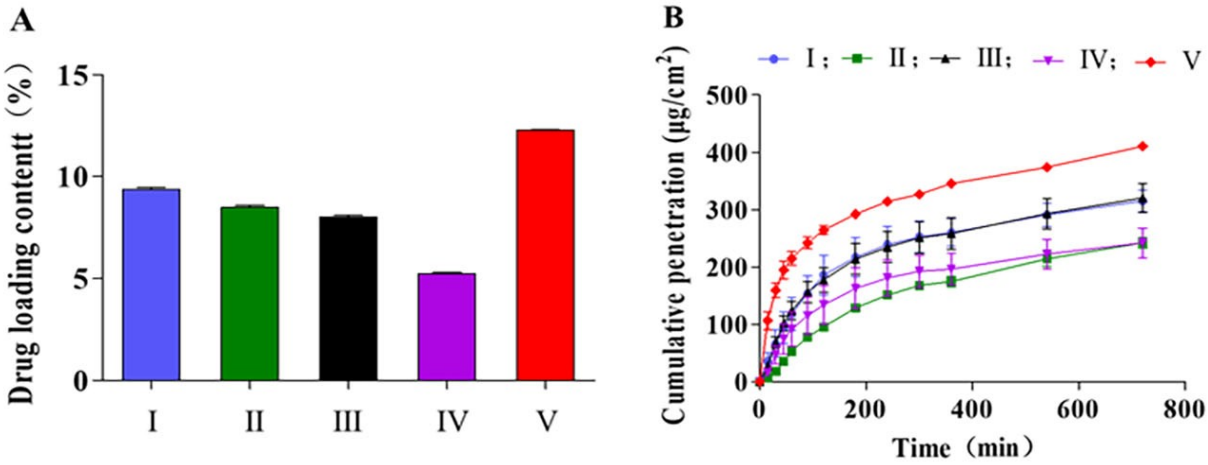

Fig. 4: (A) Drug loading of different formulations; (B) cumulative penetration of different formulations.

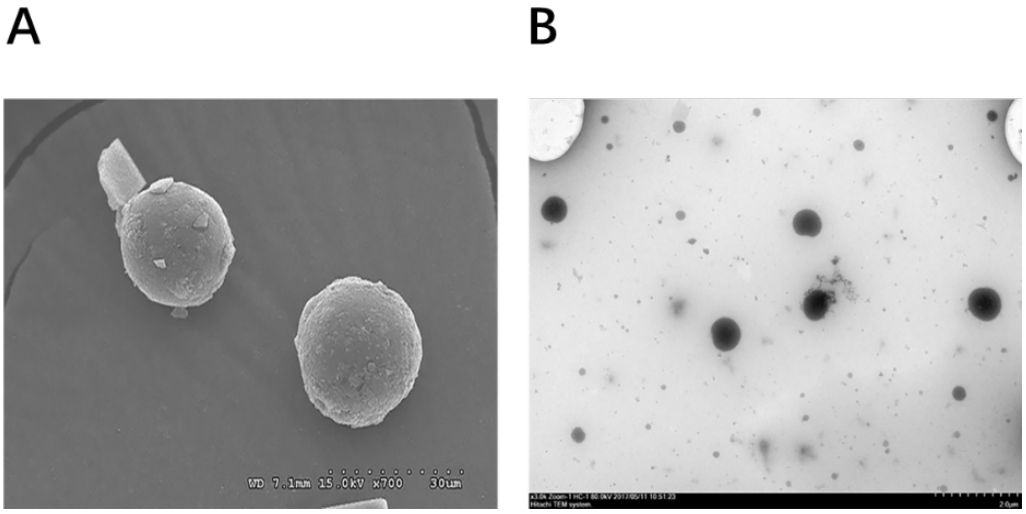

Fig. 5: Image of microcapsules observed under SEM (A) and TEM (B).

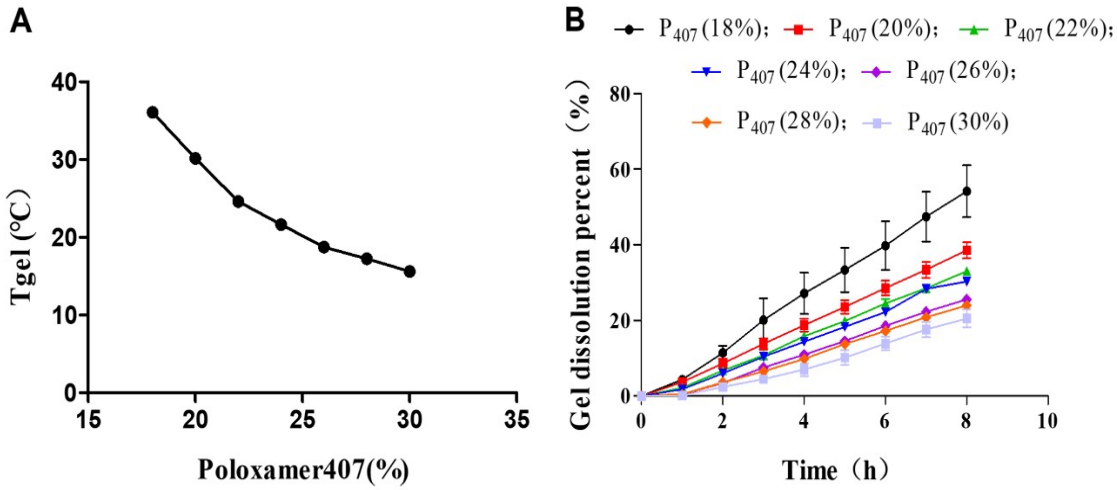

Fig. 6: Determination of (A) T_{gel} and (B) gel dissolution percent of different contents Poloxamer 407 gel.

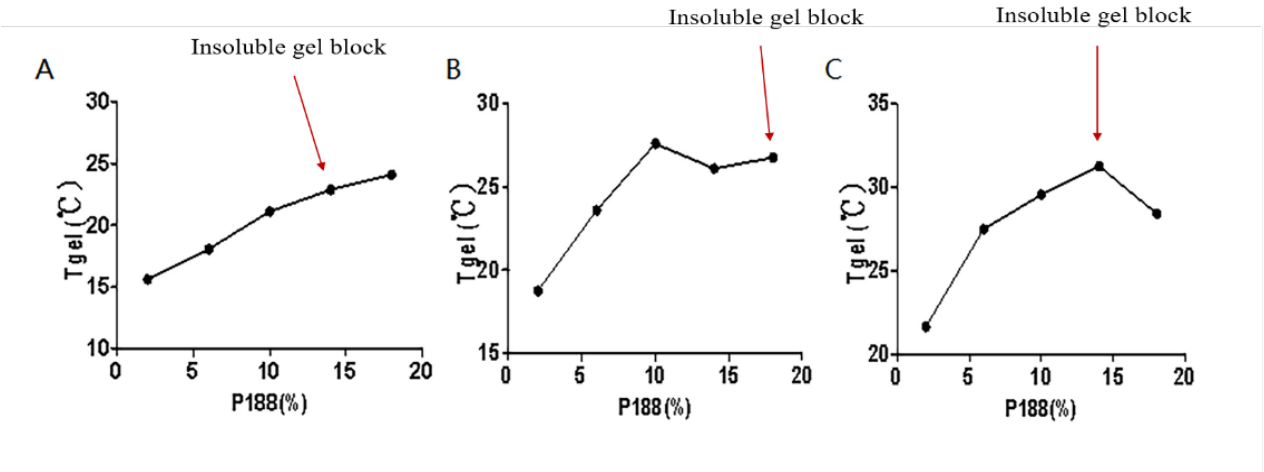

Fig. 7: Adding fixed content (A) 30% of Poloxamer 407; (B) 26% of Poloxamer 407; (C) 24% of Poloxamer 407, the effect of 2-18% P188 on the quality of T_{gel} and gel dissolution.

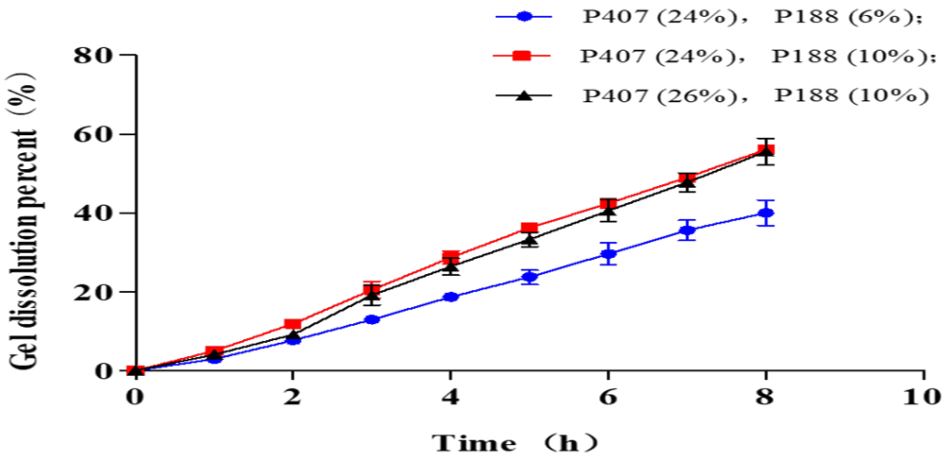

Fig. 8: Three sets of prescriptions: P407 (24%) and P188 (6%), P407 (24%) and P188 (10%), P407 (26%) and P188 (10%) gel erosion determination.

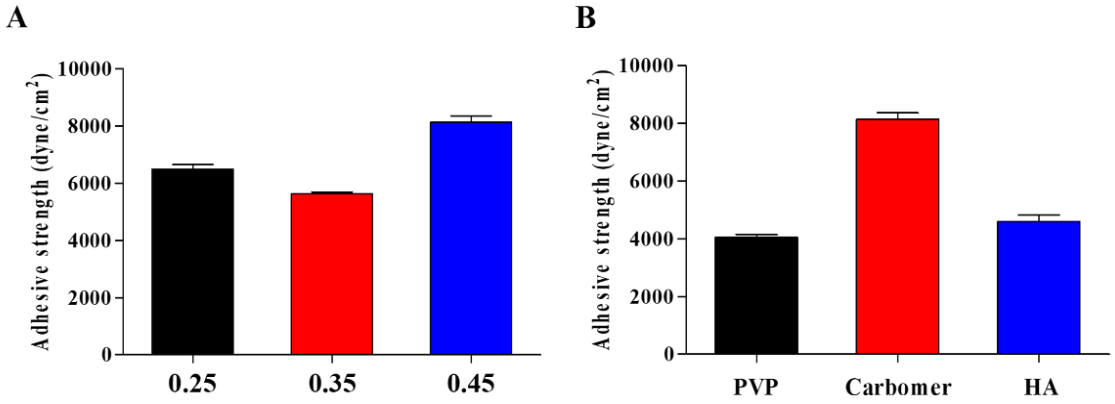

Fig. 9: (A) Screening of different content (0.25%, 0.35% and 0.45%) of bioadhesives (B) Screening of different types (PVP, Carbomer and HA) of bioadhesives.

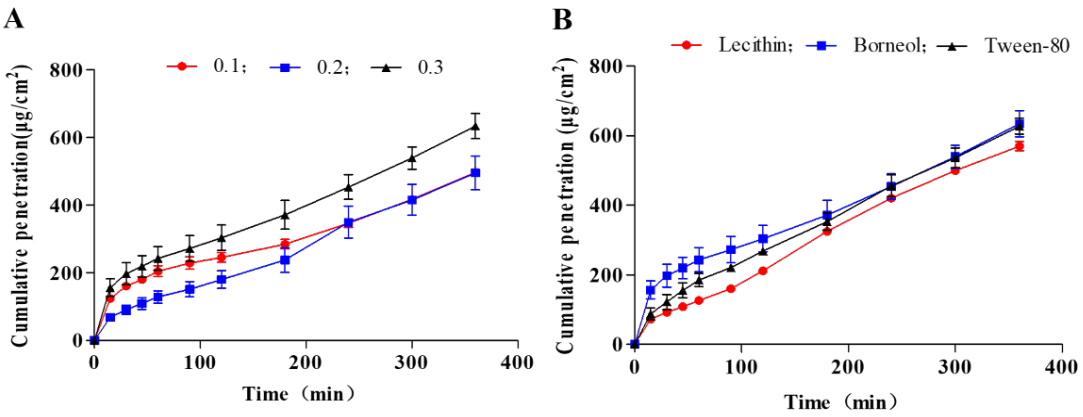

Fig. 10: (A) Screening of absorption enhancers with different content (0.1%, 0.2% and 0.3%) (B) Screening of absorption enhancers with different types (Lecithin, Borneol and Twain-80).

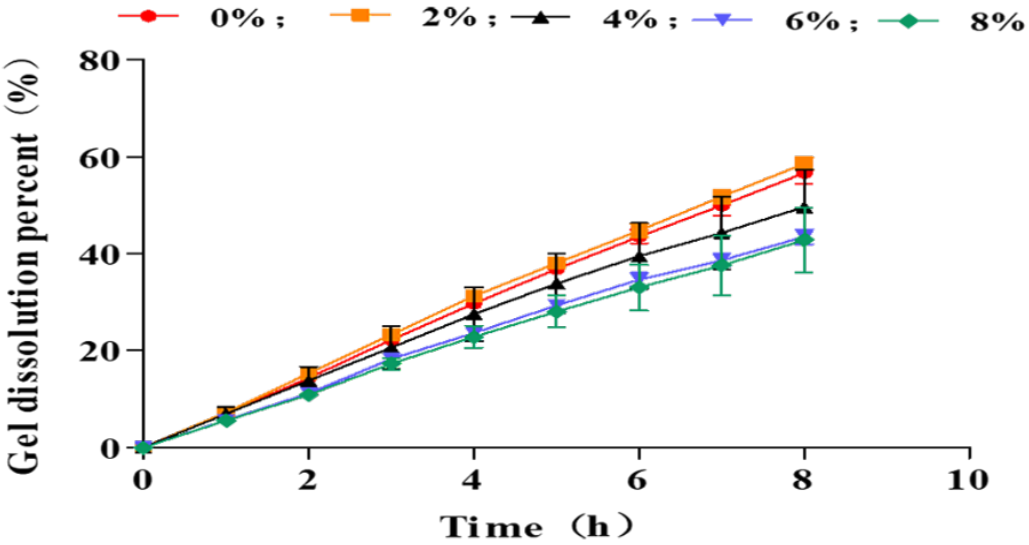

Fig. 11: Determination of the dissolution percentage of different medicines (0-8%) gel.

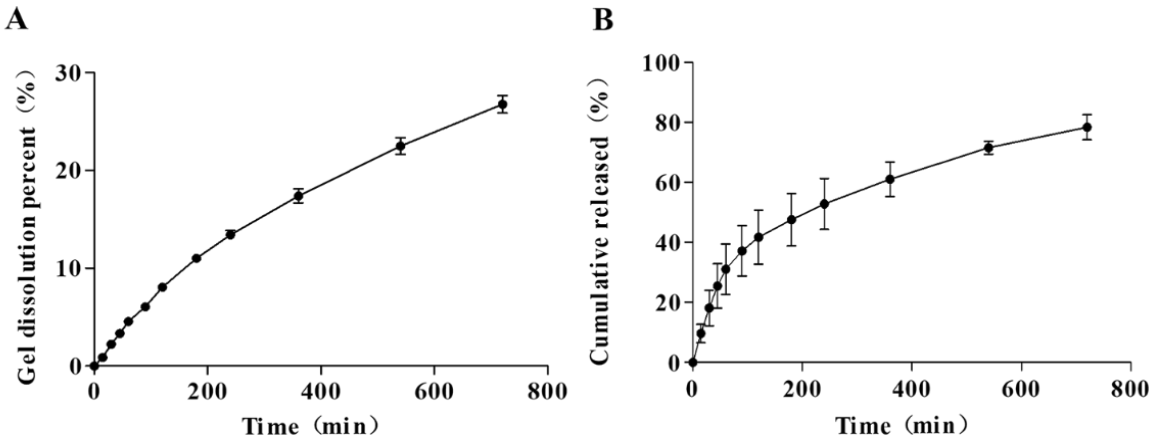

Fig. 12: (A) Gel dissolution percent; (B) Cumulative release.

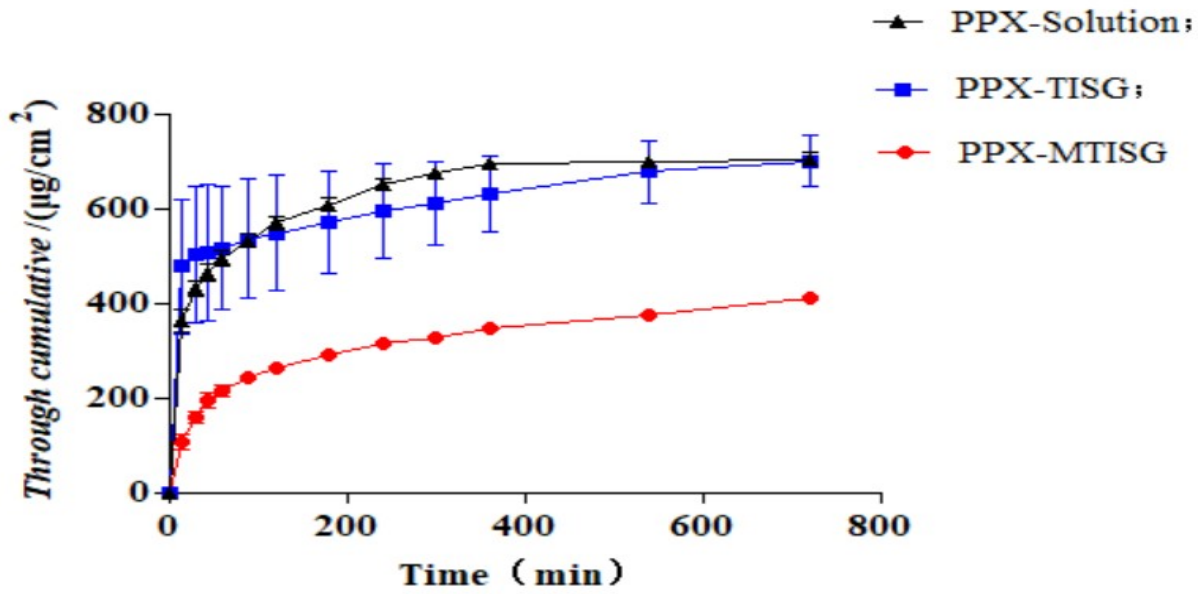

Fig. 13: In vitro cumulative penetration of formulation PPX-Solution, PPX-TISG, PPX-MTISG.

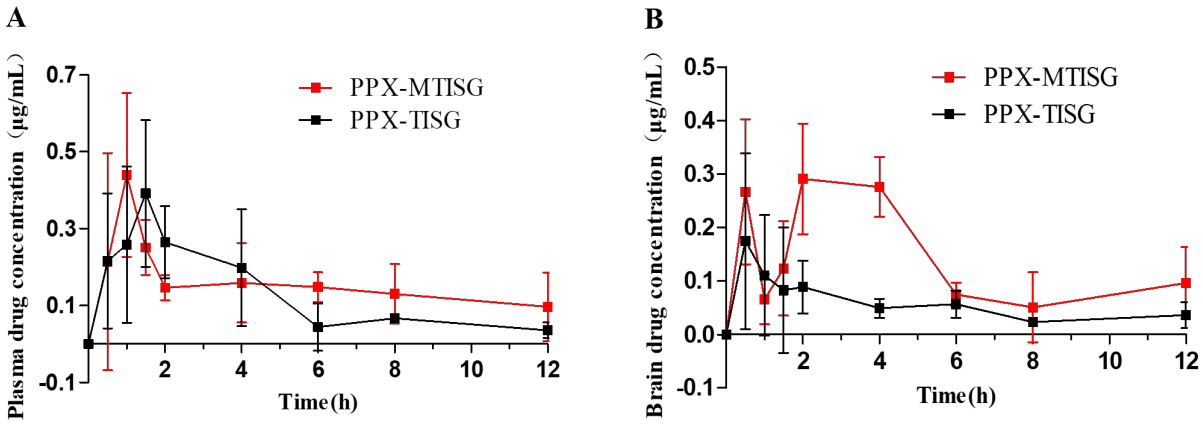

Fig. 14: (A) Plasma drug concentration; (B) Brain drug concentration.

Table 1: Formulation of PPX Microcapsules

Prescription	I	II	III	IV	V
Capsule material (g)	0.2	0.2	0.2	0.4	0.1
Span 80(%)	1	1.5	2	1.5	1.5
PPX(g)	0.05	0.05	0.05	0.05	0.05

Table 2: T_{gel} of different content of Poloxamer 407 and Poloxamer 188

Poloxamer 407 (%)	Poloxamer 188 (%)	T_{gel} (^oC)
24	6	27.50±0.08
24	10	29.57±0.12
26	10	27.60±0.24

Table 3: T_{gel} of different percent of drug *in situ* Gels

Drug (%)	0	2	4	6	8	10
T_{gel} (^oC)	30.633±0.206	32.100±0.163	31.233±0.047	30.733±0.125	28.867±0.170	27.367±0.250

Table 4: Basic properties of temperature-sensitive *in situ* Gels

T_{gel} (^oC)	t_{gel} *(S)*	PH	Viscosity (mpa.s)	Spreadability (cm)	Adhesion strength (dynes.cm^{-2})
30.9±0.455	*39.33±2.055*	3.39±0.014	241.5±2.491	6.43±0.125	2727.67±0.173

Table 5: Pharmacokinetic determination of plasma concentration and brain drug concentration

Parameters	PPX-MTISG		PPX-TISG	
	Plasma	Brain	Plasma	Brain
T_{max}/h	1.00±0.68	2.00±0.96	5.50±0.76*	1.00±0.79*
C_{max}/h	0.44±0.12	0.30±0.11	0.39±0.23*	0.18±0.10*
$T_{1/2}$/h	7.09±1.98	6.72±2.31	3.04±0.87*	5.27±1.89*
AUC (μg.h/mL)	1.89±0.99	1.57±0.93	1.58±0.89*	0.68±0.86*

Values are expressed as mean ± SD (n = 3). *p < 0.05, compared with PPX-MTISG.
T_{max}: Time required to obtain the maximum concentration, C_{max}: Maximum concentration of NTX after administration, $t_{1/2}$: The time required to half the initial concentration of the NTX in the formulation, AUC_{0-t}: Area under the curve of plasma concentration–time from time zero to the time at which the last measurable concentration is possible, $AUC_{0-\infty}$: Area under the curve of plasma concentration–time from time zero to infinity.

Determination of basic properties of temperature-sensitive in-situ gels

T_{gel} was similar to the human nasal temperature. T_{gel} was short, so it was easy to use. The pH tolerance range of the human nasal cavity is 3-10. The pH of this gel was within the tolerance range.

The in situ thermo sensitive gel prepared in this study had a viscosity of 241.5±2.5 mpa·s and could enter the nasal cavity through 23 g and 27 g needle. The length of the human nasal cavity ranges from 6.0 cm to 7.5 cm and the in situ thermo sensitive gels of this study were 6.43±0.13 cm, which indicates that it was well spread. The greater the biological adhesion, the stronger the affinity of the mucosa, the longer the retention time and the more fully the drug is absorbed. However, if the adhesive force was too large, the gel would damage the nasal mucosa. The largest adhesive force is not more than 10000 dynes·cm^{-2} (Singh et al., 2013). In this experiment, the optimum adhesive strength was (2727.67±0.17) dynes·cm^{-2}.

Determination of cumulative in vitro penetration of drugs

The results show that there is no significant difference between the gel loaded with the PPX and the PPX solution. They both have an abrupt release. In contrast, there was a significant sustained release in the *in situ* temperature-sensitive gel of PPX hydrochloride encapsulated in microcapsules with high cumulative permeation. The test could yield the same vision as the initial pilot study, where the controlled release of PPX hydrochloride was achieved by encapsulating the drug in microcapsules, which could reduce the number of doses and improve patient compliance.

Pharmacokinetic evaluations

Pharmacokinetic studies showed that the plasma concentration and brain concentration of PPX-MTISG were higher than those of PPX-MTIS after intranasal administration in rats; the drug concentration in the brain could be increased by *in situ* gel administration of PPX through temperature-sensitive microcapsules.

CONCLUSION

In this study, in order to improve the action time and targeting efficiency in the brain, PPX was loaded into a temperature-sensitive microcapsule gel. In this experiment, PPX microcapsules were prepared by the emulsifying solvent evaporation method first. The microcapsules were optimized and characterized by different drug proportions, SEM and TEM, respectively. Then the prepared temperature-sensitive gel was tested for gel temperature, gel time, gel pH, gel viscosity, etc. The successful preparation of PPX-MTISG was verified through the evaluation of the gel's spreading ability, adhesion strength, membrane free dissolution and *in vitro* permeability. The pharmacokinetic results of intranasal administration between the preparation group and the control group indicated that the developed PPX-MTISG had a longer half-life ($t_{1/2}$) and a higher concentration of the drug in the brain than the PPX-TISG. Therefore, the temperature sensitive gel of microcapsules studied in this paper can be used as an effective carrier for drug targeting to the brain and slow release.

ACKNOWLEDGEMENT

The financial assistance form Key R&D Project of Jilin Province Science and Technology Development Plan of China is gratefully acknowledged. (No. 20210204166YY).

REFERENCES

Ahmed S, Gull A, Aqil M, Danish Ansari M and Sultana Y (2019). Poloxamer-407 thickened lipid colloidal system of agomelatine for brain targeting: Characterization, brain pharmacokinetic study and behavioral study on Wistar rats. *Colloids Surf. B*, **181**: 426-436.

Akkari ACS, Papini JZB, Garcia GK, Franco M, Cavalcanti LP, Gasperini A, Alkschbirs MI, Yokaichyia F, de Paula E, Tófoli GR and de Araujo DR (2016). Poloxamer 407/188 binary thermosensitive hydrogels as delivery systems for infiltrative local anesthesia: Physico-chemical characterization and pharmacological evaluation. *Mater. Sci. Eng. C*, **68**: 299-307.

Bagci N, Bayindir ZS, Inal O, Altanlar N and Yuksel N (2020). Development and *in vitro* evaluation of nifedipine gel formulations for anorectal applications. *Curr. Drug Delivery*, **17**(2): 126-139.

Bah MG, Bilal HM and Wang J (2020). Fabrication and application of complex microcapsules: A review. *Soft Matter*, **16**(3): 570-590.

Barakat NS, Omar SA and Ahmed AA (2006). Carbamazepine uptake into rat brain following intra-olfactory transport. *J. Pharm. Pharmacol.*, **58**(1): 63-72.

Choi JE, Kim KR, Noh Y, Chung WH, Cho YS, Chung SK, Dhong HJ and Kim HY (2017). Intranasal distribution and clearance of thermoreversible gel in an animal model. *Int. Forum Allergy Rhinol*, **7**(7): 705-711.

Colombo M, Figueiró F, de Fraga Dias A, Teixeira HF, Battastini AMO and Koester LS (2018). Kaempferol-loaded mucoadhesive nanoemulsion for intranasal administration reduces glioma growth *in vitro*. *Int. J. Pharm.,* **543**(1-2): 214-223.

Dahlizar S, Futaki M, Okada A, Kadhum WR, Todo H and Sugibayashi K (2018). Design of a topically applied gel spray formulation with ivermectin using a novel low molecular weight gelling agent, palmitoyl-glycine-histidine, to treat scabies. *Chem. Pharm. Bull.*, **66**(3): 327-333.

Dai HH, Li XD, Wei AC, Wang XD and Wang DY (2020). Characterization and oxidative stability of cold-pressed sesame oil microcapsules prepared by complex coacervation. *J. Oleo Sci.*, **69**(7): 685-692.

Dorsey ER, Sherer T, Okun MS and Bloem BR (2018). The emerging evidence of the parkinson pandemic. *J. Parkinson's Dis.*, **8**(s1): S3-S8.

Elsenosy FM, Abdelbary GA, Elshafeey AH, Elsayed I and Fares AR (2020). Brain targeting of duloxetine HCL via intranasal delivery of loaded cubosomal gel: *in vitro* characterization, *ex vivo* permeation and *in vivo* biodistribution studies. *Int. J. Nanomed.*, **15**: 9517-9537.

Feng J, Yang G, Zhang S, Liu Q, Jafari SM and McClements DJ (2018). Fabrication and characterization of β-cypermethrin-loaded PLA microcapsules prepared by emulsion-solvent evaporation: loading and release properties. *Environ. Sci. Pollut. Res.*, **25**(14): 13525-13535.

Giuliano E, Paolino D, Fresta M and Cosco D (2018). Mucosal Applications of Poloxamer 407-Based Hydrogels: An Overview. *Pharmaceutics*, **10**(3): 159.

Gonçalves J, Bicker J, Gouveia F, Liberal J, Oliveira RC, Alves G, Falcão A and Fortuna A (2019). Nose-to-brain delivery of levetiracetam after intranasal administration to mice. *Int. J. Pharm.*, **564**: 329-339.

Gu F, Fan H, Cong Z, Li S, Wang Y and Wu C (2020). Preparation, characterization and *in vivo* pharmacokinetics of thermosensitive in situ nasal gel of donepezil hydrochloride. *Acta Pharmacol. Sin.*, **70**(3): 411-422.

Jain SK, Jain AK and Rajpoot K (2020). Expedition of Eudragit® polymers in the development of novel drug delivery systems. *Curr. Drug Delivery*, **17**(6): 448-469.

Jin R, Moreira Teixeira LS, Dijkstra PJ, Karperien M, van Blitterswijk CA, Zhong ZY and Feijen J (2009). Injectable chitosan-based hydrogels for cartilage tissue engineering. *Biomaterials*, **30**(13): 2544-2551.

Liu S, Long Y, Yu S, Zhang D, Yang Q, Ci Z, Cui M, Zhang Y, Wan J, Li D, Shi A, Li N, Yang M and Lin J (2021). Borneol in cardio-cerebrovascular diseases: Pharmacological actions, mechanisms and therapeutics. *Pharmacol Res*, **169**: 105627.

Liu S, Yang S and Ho PC (2018). Intranasal administration of carbamazepine-loaded carboxy-methyl chitosan nanoparticles for drug delivery to the

brain. *Asian. J. Pharm. Sci.*, **13**(1): 72-81.

Liu Y, Liu W, Xiong S, Luo J, Li Y, Zhao Y, Wang Q, Zhang Z, Chen X and Chen T (2020). Highly stabilized nanocrystals delivering Ginkgolide B in protecting against the Parkinson's disease. *Int. J. Pharm.*, **577**: 119053.

Machado HA, Abercrombie JJ, You T, Deluca PP and Leung KP (2013). Release of a wound-healing agent from PLGA microspheres in a thermosensitive gel. *Biomed Res. Int.*, 2013: 387863.

Mahajan HS and Gattani SG (2009). Gellan gum based microparticles of metoclopromide hydrochloride for intranasal delivery: Development and evaluation. *Chem. Pharm. Bull.*, **57**(4): 388-392.

Mahajan HS, Mahajan MS, Nerkar PP and Agrawal A (2014). Nanoemulsion-based intranasal drug delivery system of saquinavir mesylate for brain targeting. *Drug Deliv.*, **21**(2): 148-154.

Matsuho M, Kubota R, Asayama S and Kawakami H (2017). Lactoferrin-modified nanoparticles loaded with potent antioxidant Mn-porphyrins exhibit enhanced antioxidative activity *in vitro* intranasal brain delivery model. *J. Mater. Chem. B*, **5**(9): 1765-1771.

McCormick PN, Fletcher PJ, Wilson VS, Browne JD, Nobrega JN and Remington GJ (2015). Low dose pramipexole causes D3 receptor-independent reduction of locomotion and responding for a conditioned reinforcer. *Neuropharmacology*, **89**: 225-231.

Merkus FW, Verhoef JC, Schipper NG and Marttin E (1998). Nasal mucociliary clearance as a factor in nasal drug delivery. *Adv. Drug Delivery Rev.*, **29**(1-2): 13-38.

Nižić L, Potaś J, Winnicka K, Szekalska M, Erak I, Gretić M, Jug M and Hafner A (2020). Development, characterisation and nasal deposition of melatonin-loaded pectin/hypromellose microspheres. *Eur. J. Pharm. Sci.*, **141**: 105115.

Nižić L, Ugrina I, Špoljarić D, Saršon V, Kučuk MS, Pepić I and Hafner A (2019). Innovative sprayable in situ gelling fluticasone suspension: Development and optimization of nasal deposition. *Int. J. Pharm.*, **563**: 445-456.

Patil S and Murthy RSR (2006). Preparation and *in vitro* evaluation of mucoadhesive Chitosan microspheres of Amlodipine Besylate for nasal administration. *Indian J. Pharm. Sci.*, **68**(1): 64.

Pidaparthi K and Suares D (2017). Comparison of nanoemulsion and aqueous mcelle systems of paliperidone for intranasal delivery. *AAPS PharmSciTech.*, **18**(5): 1710-1719.

Prajapati SK, Tripathi P, Ubaidulla U and Anand V (2008). Design and development of gliclazide mucoadhesive microcapsules: *in vitro* and *in vivo* evaluation. *AAPS PharmSciTech.*, **9**(1): 224-230.

Radhakrishnan DM and Goyal V (2018). Parkinson's disease: A review. *Neurol India*, **66**(7): 26.

Rassu G, Soddu E, Cossu M, Brundu A, Cerri G, Marchetti N, Ferraro L, Regan RF, Giunchedi P, Gavini E and Dalpiaz A (2015). Solid microparticles based on chitosan or methyl-β-cyclodextrin: A first formulative approach to increase the nose-to-brain transport of deferoxamine mesylate. *J. Controlled Release*, **201**: 68-77.

Salunke SR and Patil SB (2016). Ion activated i*n situ* gel of gellan gum containing salbutamol sulphate for nasal administration. *Int. J. Biol. Macromol.*, **87**: 41-47.

Samii A, Nutt JG and Ransom BR (2004). Parkinson's disease. *Lancet*, **363**(9423): 1783-1793.

Serralheiro A, Alves G, Fortuna A and Falcão A (2015). Direct nose-to-brain delivery of lamotrigine following intranasal administration to mice. *Int. J. Pharm.*, **490**(1-2): 39-46.

Shaohua, Sun, Hui, Cao, Haijia, SuTianwei and Tan (2009). Preparation and characterization of a novel injectable in situ cross-linked hydrogel. *Polymer Bulletin*, **62**(5): 699-711.

Shen Y, Wang Y, Zhao X, Sun C, Cui B, Gao F, Zeng Z and Cui H (2017). Preparation and physicochemical characteristics of thermo-responsive emamectin benzoatemicrocapsules. *Polymers*, **9**(9): 418.

Singh RM, Kumar A and Pathak K (2013). Thermally triggered mucoadhesive in situ gel of loratadine: β-cyclodextrin complex for nasal delivery. *AAPS PharmSciTech*, **14**(1): 412-424.

Teaima MH, El Mohamady AM, El-Nabarawi MA and Mohamed AI (2020). Formulation and evaluation of niosomal vesicles containing ondansetron HCL for trans-mucosal nasal drug delivery. *Drug Dev. Ind. Pharm.*, **46**(5): 751-761.

Wang F, Yang Z, Liu M, Tao Y, Li Z, Wu Z and Gui S (2020). Facile nose-to-brain delivery of rotigotine-loaded polymer micelles thermosensitive hydrogels: *In vitro* characterization and *in vivo* behavior study. *Int. J. Pharm.*, **577**: 119046.

Wang Y, Hu R, Guo Y, Qin W, Zhang X, Hua L and Yang Y (2021). Preparation, evaluation and *in vitro* release of chitosan-alginate tanshinone self-microemulsifying sustained-release microcapsules. *Technol Health Care*, **29**(4): 687-695.

Zarrintaj P, Ramsey JD, Samadi A, Atoufi Z, Yazdi MK, Ganjali MR, Amirabad LM, Zangene E, Farokhi M, Formela K, Saeb MR, Mozafari M and Thomas S (2020). Poloxamer: A versatile tri-block copolymer for biomedical applications. *Acta Biomater*, **110**: 37-67.

Zhan Y, Du YT, Yang ZZ, Zhang CL and Qi XR (2019). Preparation and characterization of paclitaxel microspheres in situ gel and its antitumor efficacy by local injection. *Beijing Da Xue Xue Bao Yi Xue Ban*, **51**(3): 477-486.